Dynamics of Sine-Gordon Solitons in the Annular Josephson Junction

A. V. Ustinov,[a] T. Doderer, R. P. Huebener, N. F. Pedersen,[b] B. Mayer, and V. A. Oboznov[c]

Lehrstuhl Experimentalphysik II, University of Tuebingen, D-7400 Tuebingen, Germany

(Received 12 March 1992; revised manuscript received 22 June 1992)

The annular Josephson junction allows for the study of undisturbed soliton (fluxon) motion in the absence of collisions. With new experimental methods and design we have realized for the first time a fully controllable way of introducing individual fluxons or antifluxons into such a system. This has allowed us to study multisoliton behavior and to make a comparison with existing soliton-chain perturbation theory. An unforeseen crossover in the dynamical behavior at high velocities is tentatively interpreted in terms of soliton bunching.

PACS numbers: 74.50.+r, 03.40.Kf, 74.60.Ge

Solitons, particularly sine-Gordon solitons, play an important role in physics as examples of nonlinear wave motion [1,2]. This paper emphasizes new results for the ideal experimental system—the annular Josephson junction [3,4]. With new experimental methods and junction design we have realized for the first time a fully controllable way of introducing individual fluxons or antifluxons into such a system. This has allowed us to study multisoliton behavior and to make a comparison with existing soliton-chain perturbation theory.

The system discussed here is described by the perturbed sine-Gordon equation [1–3],

$$\varphi_{xx}-\varphi_{tt}=\sin\varphi+\alpha\varphi_t-\beta\varphi_{xxt}+\gamma\,, \tag{1}$$

where $\varphi(x,t)$ is the space- and time-dependent superconducting phase difference. The spatial coordinate x is normalized to the Josephson penetration depth λ_J, and the time t to the inverse plasma frequency ω_0^{-1}, α and β are the dissipation coefficients, and γ is the bias current.

In the case of the conventional topology of a long Josephson junction, a moving soliton cannot avoid collisions with other solitons and the junction boundaries. This strongly complicates the analysis and interpretation of the experimental data. In the annular junction [3,4] the boundary conditions for Eq. (1) are periodic, so we may avoid collisions and study in a controllable way the motion of individual fluxons. New sample design and experimental methods give the present work a major advantage over previous works [3,4], and lead to new results.

In order to trap solitons we have applied the technique of low-temperature scanning electron microscopy [5]. We used Nb-Pb annular Josephson tunnel junctions which were very close to the classical geometry [3,4] [Fig. 1(a)]. The most important improvement was the use of a SiO insulating window. The tunnel barrier was formed in the area between two SiO rings. A spatially resolved investigation showed high homogeneity of the tunnel barrier [Fig. 1(b)].

Annular junctions of two typical dimensions with an inner ring radius of 150 and 100 μm and with a tunnel barrier ring width of 10 and 20 μm, respectively, were used. The critical current of the junction, $I_c=3.3$ mA, was only about (15–20)% smaller than the ideal value for a small junction, which implies that the self-field effects are negligible. The critical current density was about 40 A/cm^2, which corresponds to $\lambda_J\approx 70$ μm.

The sample was attached to the top side of a sapphire disk using high-thermal-conductivity glue. During the experiments the bottom side of the sapphire disk was in direct contact with liquid He, whereas the top side carrying the Josephson junctions was exposed to the vacuum of the scanning electron microscope. The sample temperature during the measurements was about 5 K. A heater could be used to remove trapped magnetic flux from the sample. The external magnetic field H_z was applied in the direction perpendicular to the substrate plane. The I-V curves were measured by a model 181 Keithley nanovoltmeter.

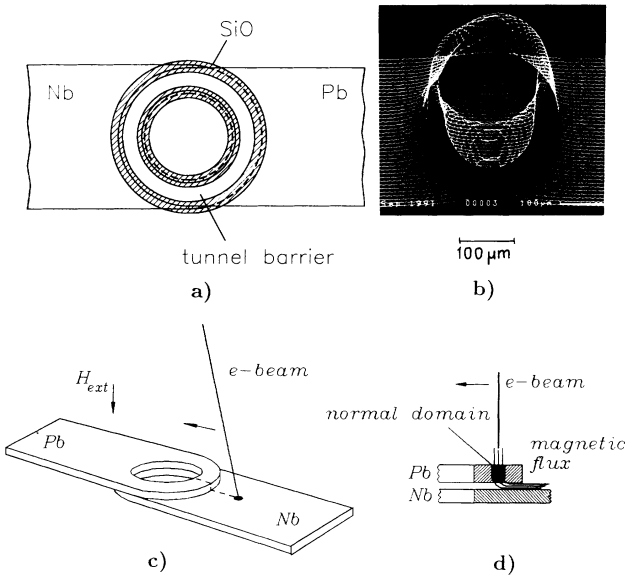

FIG. 1. (a) An improved annular Josephson-junction geometry. (b) Spatial distribution of the subgap conductivity obtained by scanning the electron beam across the annular junction. (c) A sketch of the annular junction with the electron beam moving across the substrate. (d) The cross section of the junction in the region shown by the dashed line in (c) at the moment when the beam focus is in the junction area.

The focused electron beam was used for trapping magnetic flux quanta in the annular junctions. Crossing of the top electrode by the electron beam focus resulted in trapping the magnetic flux in the tunnel barrier [Fig. 1(c)]. This was due to the local heating of the sample by the beam. A normal domain carrying the magnetic flux was moved across the Pb film together with the electron beam focus as shown in Fig. 1(d). The trapping procedure was performed without any bias current passing through the junction. The details of this technique are presented elsewhere [4].

Figure 2(a) shows the experimental I-V curves for the trapping of solitons in the annular Josephson junction obtained by a sequential crossing of the junction with the electron beam. The resonant soliton steps corresponding to different numbers n of unipolar solitons are observed. The I-V curves are symmetrical with respect to the origin. The voltages of the steps are quantized as expected, according to the formula [2] $V_n = n\Phi_0\bar{c}/L$, where Φ_0 is the magnetic flux quantum, $\bar{c}$ is the maximum velocity of the electromagnetic waves in the junction, and L is the junction circumference. At the step voltage V_n the solitons move as relativistic particles with velocity close to $\bar{c}$.

With properly adjusted electron beam parameters the magnetic-flux-trapping procedure worked quite reproducibly. The electron beam focus was placed on the Nb film outside the junction and moved towards the junction [Fig. 1(c)]. After crossing the junction area the beam was stopped in the opening inside the ring and then blanked. In most cases such a procedure resulted in trapping one soliton in the junction. When the process was repeated, voltage steps with increasing number n were observed. Reversal of the magnetic field H_z during the trapping sequence resulted in a decrease of the step number. By heating the whole substrate above the critical temperature of the superconducting films it was easy to remove all trapped flux from the junction.

If solitons are trapped in an ideally homogeneous annular junction, theoretically the nondissipative critical current I_c should be equal to zero. This is perfectly fulfilled for all the curves in Fig. 2(a) and represents a good proof for the high homogeneity of our junctions. Sometimes during the trapping procedure a certain critical current [typically (5–10)% of I_c] was observed. A redistribution of the magnetic flux occasionally trapped in the electrodes under the influence of the electron beam probably took place. Figure 2(b) shows as an example the first voltage step (A) obtained as described above. This step displays a critical current of about 50 μA. Curves B and C show the same step after irradiation of the sample area around the junction by a defocused beam with lower power. For curve C the critical current has been reduced to an insignificant level.

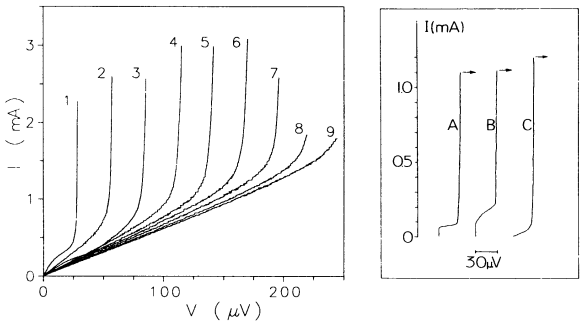

FIG. 2. (a) I-V curves corresponding to the sequential trapping of solitons in the annular Josephson junction. The numbers indicate the number of solitons trapped. (b) The modification of the first soliton step by irradiation of the area around the junction with a defocused electron beam.

It is essential to emphasize the distinct difference of the steps which we have observed from those of a linear long junction, where the steps may also arise from cavity mode excitations. This mechanism is known as an alternative to the soliton-type one. A cavity mode may be excited only if there is a strong inhomogeneity like an open boundary of the junction. For the cavity mode excitations the steps are typically very steep and they all approach the same limiting curve as $I \to 0$. In our case, except for very large step number n, the slope of the I-V curves at small I changes with n, which agrees with the soliton picture. Another characteristic of higher cavity mode steps in linear junctions is a negative differential resistance, which is often observed at the bottom of the steps. We did not observe any behavior like this for the steps reported in this paper. However, sometimes we also observed this feature in our annular junctions (in the form of unstable switching from the lower part of a step to higher voltages) when parasitic magnetic flux was trapped in the films.

We have found the soliton steps in the I-V curve to be highly stable. As a result of electromagnetic interference and external noise during the measurements in the scanning electron microscope, current jumps from the soliton step to the gap voltage and back were occasionally observed but only at high currents close to the top of the step. At lower currents we found the soliton steps to be *globally stable dynamical states* of the system and jumps to the gap voltage never occurred. This is in contradiction to conventional long Josephson junctions, where the soliton steps are rather unstable. The curves in Fig. 2(a) show only globally stable parts.

Figure 3(a) shows the lower parts of some steps from Fig. 2(a). With increasing step number the steps asymptotically approach the McCumber curve. The multisoliton states for the perturbed sine-Gordon system with periodic boundary conditions was analyzed by Marcus and Imry [6]. They obtained the I-V characteristics in the following form:

$$\gamma = \frac{4a}{\pi}\frac{E(k)}{k}\frac{v}{(1-v^2)^{1/2}}, \quad \xi = \frac{L}{n\lambda_J} = 2kK(k), \qquad (2)$$

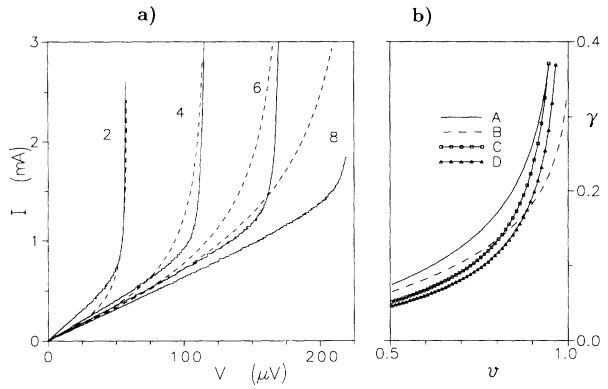

FIG. 3. (a) Lower parts of some steps from Fig. 2(a) (solid lines). The dashed curves represent a fit using Eq. (2). (b) Theoretical I-V curve (2) with $\alpha=0.1$ (A), the same curve when taking into account the finite width of the ring (B), β losses with $\alpha=0.05$ and $\beta=0.05$ (C), and taking into account both the β losses and the finite width of the ring (D).

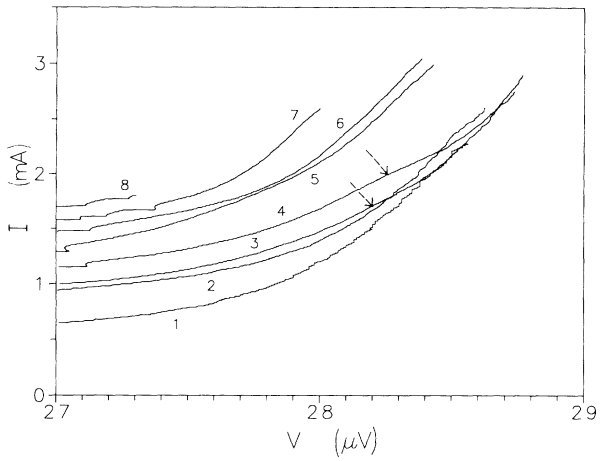

FIG. 4. The detailed comparison of the high-current parts of the scaled soliton steps in a magnified voltage scale (the voltage of the nth step is divided by n). The arrows show approximately the crossover regions where the steps with $n=3$ and $n=4$ start to shift to higher voltages.

where $K(k)$ and $E(k)$ are the complete elliptic integrals of the first and second kind with modulus k, respectively, and v is the soliton velocity normalized to $\bar{c}$. The dashed curves in Fig. 3(a) show a two-parameter fit of Eq. (2) to the experimental I-V curves (solid lines). The tendency to reach an asymptotic linear slope with increasing number n of solitons is similar both for theory and experiment. However, in the crossover region between the linear slope and the relativistic vertical part of the steps deviations between experiment and theory are evident. We suggest two reasons that can explain this discrepancy. First, because of the finite width of the junction the moving soliton has a difference in velocity at the outer and the inner radius of the ring. This difference is relatively large [about (8–20)% for our junctions] and is drastic at high velocities. The corresponding correction to the I-V curve can be calculated by averaging the velocity-dependent losses over the width of the soliton [7]. Figure 3(b) shows the shape of the I-V curve modified by taking into account a finite width of the ring $\Delta R/R=0.2$ (curve B). Second, Eq. (2) does not include the surface losses corresponding to the well known [8] β term in Eq. (1). Curve C shows the modified shape of the I-V curve obtained by taking into account the β losses. Curve D corresponds to the case when both the β losses and the finite width of the ring are taken into account. Although we are not attempting a detailed fit, we see that these corrections improve the agreement between theory and experiment.

A new feature predicted in Ref. [6] was the increase of the step height I_n (even exceeding I_c) with the step number n. We note a similar tendency for steps 4, 5, and 6 in Fig. 2(a). To our knowledge this has never been observed experimentally before. In conventional long linear Josephson junctions the step height always decreases with increasing n. We believe that this difference between linear and annular junctions is due to the global stability of the soliton steps in the annular system.

Figure 4 shows the current plotted versus the voltage per fluxon V_n/n and displays the top parts of the steps in a magnified voltage scale. Since V_n/n is proportional to the average fluxon velocity v, we can compare the dependence of v on the external driving force $I\sim\gamma$ for different fluxon densities. With increasing step number a crossover in the step voltage is clearly seen. At high current I the normalized voltage V_n/n for the steps with $n>4$ is considerably lower than for the steps with smaller n. In principle, a certain monotonic decrease of v with increasing n is expected [6]. It can be explained as an increase of the effective damping parameter $\alpha E(k)$ as k decreases with increasing n. However, it is evident from Fig. 4 that the changes of the curves with increasing n cannot be described by only a smooth one-parameter scaling. In particular, at certain fluxon velocities (shown by arrows in Fig. 4) the steps with $n=3$ and $n=4$ display a shift to higher voltages, which is not expected by theory [6].

We suggest the following explanation of this crossover at high velocities. As known from computer simulations [8], the dissipation due to the β losses at high velocity generates an effective attraction between unipolar solitons and results in bunching in a localized soliton train moving in the junction. This bunching effect breaks the symmetry in the annular system and "helps" the chain of solitons to overcome the dissipative losses. Their average velocity then becomes higher than that of a single soliton at the same bias current. Malomed [9] has recently shown that in an annular system the threshold velocity of soliton bunching increases with increasing soliton number n. The experimental curve for $n=4$ displays the voltage increase at a soliton velocity which is higher than that for $n=3$, in agreement with the theoretical prediction. This

explanation is relevant for the case $\xi \gg 1$ when solitons are well separated. Thus, it is not surprising that we do not see any distinct crossover for $n > 4$, because in those cases ξ is of the order of 1 and the single-soliton behavior cannot be expected.

We are grateful to M. Cirillo, A. Davidson, B. A. Malomed, K. Nakajima, S. Pagano, R. D. Parmentier, S. Sakai, A. C. Scott, and I. V. Vernik for stimulating discussions. We also thank V. Kaplunenko for the layout design using his "Z"-topological compiler program and A. Goncharov for manufacturing of the photomasks. A.V.U. gratefully acknowledges the support of the Alexander von Humboldt Stiftung. This work was also supported by a grant of the Deutsche Forschungsgemeinschaft.

[a]Present address: Physics Laboratory I, Technical University of Denmark, DK-2800 Lyngby, Denmark. Permanent address: Institute of Solid State Physics, Russian Academy of Sciences, Chernogolovka, Moscow district, 142432, Russia.

[b]Permanent address: Physics Laboratory I, Technical University of Denmark, DK-2800 Lyngby, Denmark.

[c]Permanent address: Institute of Solid State Physics, Russian Academy of Sciences, Chernogolovka, Moscow district, 142432, Russia.

[1] D. W. McLaughlin and A. C. Scott, Phys. Rev. A **18**, 1652 (1978).

[2] N. F. Pedersen, in *Solitons, Modern Problems in Condensed Matter Sciences*, edited by A. A. Maradudin and V. M. Agranovich (North-Holland, Amsterdam, 1986), p. 486.

[3] A. Davidson, B. Dueholm, B. Kryger, and N. F. Pedersen, Phys. Rev. Lett. **55**, 2059 (1985); A. Davidson, B. Dueholm, and N. F. Pedersen, J. Appl. Phys. **60**, 1447 (1986).

[4] A. V. Ustinov, T. Doderer, B. Mayer, R. P. Huebener, and V. A. Oboznov, Europhys. Lett. **19**, 63 (1992).

[5] R. P. Huebener, Rep. Prog. Phys. **47**, 175 (1984).

[6] P. M. Marcus and Y. Imry, Solid State Commun. **33**, 345 (1980).

[7] A. V. Ustinov, T. Doderer, R. P. Huebener, and N. F. Pedersen (unpublished).

[8] W. J. Johnson, Ph.D. thesis, University of Wisconsin, 1968 (unpublished); A. Davidson, N. F. Pedersen, and S. Pagano, Appl. Phys. Lett. **48**, 1306 (1986).

[9] B. A. Malomed (unpublished).

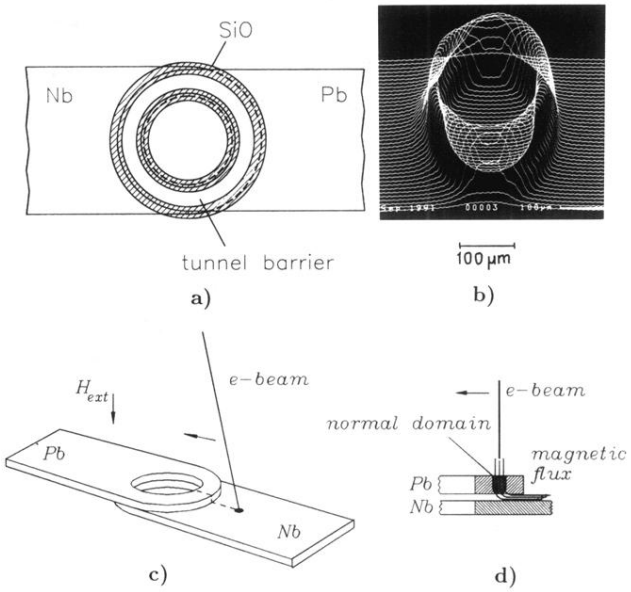

FIG. 1. (a) An improved annular Josephson-junction geometry. (b) Spatial distribution of the subgap conductivity obtained by scanning the electron beam across the annular junction. (c) A sketch of the annular junction with the electron beam moving across the substrate. (d) The cross section of the junction in the region shown by the dashed line in (c) at the moment when the beam focus is in the junction area.